Accepted Manuscript

Wheat germ thermal treatment in fluidised bed. Experimental study and mathematical modelling of the heat and mass transfer

Renato D. Gili, R. Martín Torrez Irigoyen, M. Cecilia Penci, Sergio A. Giner, Pablo D. Ribotta

Please cite this article as: Gili, R.D., Torrez Irigoyen, R.Martí., Penci, M.C., Giner, S.A., Ribotta, P.D., Wheat germ thermal treatment in fluidised bed. Experimental study and mathematical modelling of the heat and mass transfer, *Journal of Food Engineering* (2017), doi: 10.1016/j.jfoodeng.2017.09.029.

1 **Wheat germ thermal treatment in fluidised bed. Experimental study and**
2 **mathematical modelling of the heat and mass transfer**

3

4 Renato D. Gili[1,3], R. Martín Torrez Irigoyen[2], M. Cecilia Penci[1,3], Sergio A. Giner[2],

5 Pablo D. Ribotta[1,3]

6 (1) Instituto de Ciencia y Tecnología de Alimentos Córdoba (ICYTAC), CONICET-

7 UNC, Argentina.

8 (2) Centro de Investigación y Desarrollo en Criotecnología de Alimentos (CIDCA),

9 CONICET-UNLP, Argentina.

10 (3) Instituto de Ciencia y Tecnología de los Alimentos (ICTA), FCEFyN-UNC, Av.

11 Vélez Sarsfield 1611, Córdoba, Argentina

12 Corresponding author: Pablo D. Ribotta; Phone Number: +54-351-5353755 int.

13 17141

14 E-mail address: pdribotta@unc.edu.ar; ORCID: https://orcid.org/0000-0001-7883-

15 8856

16

17

18 **Abstract**

19

20 Wheat germ is an abundant by-product of the milling industry, it has excellent

21 nutritional qualities and high tocopherols content. The aim of this work was to study

22 the kinetics of wheat germ drying in fluidised thin-layers by applying analytical

23 solutions of the diffusion equation. Also, was determined the effective heat transfer

24 coefficient by solving the macroscopic energy balance to contribute with the design

25 and optimization of a thermal treatment for this product. Four air temperatures were

26 studied in this work, 90-150°C. The heat transfer coefficients were estimated using

27 experimental drying rates (7.87 to 16.55 $W/m^2°C$). The effective diffusion coefficient

28 for water was determined to vary from 3.22×10^{-11} to 2.38×10^{-10} m^2/s. The

29 analytical solution for short times was not suitable for this high temperature process.

30 Values of diffusion coefficient and activation energy (39.27 kJ/mol) were within the

31 ranges expected for food drying at elevates temperatures.

32

33 **Key words**

34 Wheat germ; Fluidization; Mathematical modelling, Effective diffusion coefficient,

35 Effective heat transfer coefficient.

36

37 **Notation**

38

39   A_v Specific particle surface, m^{-1}

40   a_w Water activity

41   C_p Specific heat of wheat germ particle, J kg^{-1} (dry matter) °C^{-1}

42   D_{eff} Effective diffusion coefficient of water in wheat germ, m^2 s^{-1}

43   D_{∞} Preexponential factor in Arrhenius equation for water diffusivity, m^2 s^{-1}

44   E_a Activation energy kJ mol^{-1}

45   h_t Effective heat transfer coefficient, W m^{-2} °C^{-1}

46   L_0 Half part of particle thickness at initial moisture content, m

47   L_g Heat of desorption of water in the particle, J kg^{-1}

48   L_w Heat of vaporization of pure water, J kg^{-1}

49   M_w Molar mass of water, kg kmol^{-1}

50   p_v Vapor pressure of water in particles, Pa

51   p_s Saturation vapor pressure of pure water, Pa

52   p_{va} Partial pressure of vapor in air, Pa

53   p_{vs} Vapor pressure of water in the particle surface, Pa

54   R Universal gas constant, 8.314, kJ kmol^{-1} K^{-1}

55   S_y Standard deviation of the estimate

56   t Time, s

57   T   Particle temperature, °C

58   W Wheat germ moisture content, kg water/ kg dry matter

59   W_{ad} Dimensionless wheat germ moisture content

60

Greek symbols

61   π Constant

62   ρ_p Particle density, kg m^{-3}

63   ρ_s Dry matter density of wheat germ, kg m^{-3}

64

Subscripts

65   0   Initial

66   e Equilibrium

67   exp Experimental value

68   K Kelvin

69   l Local

70   m Average

71   s Surface

72   sim Simulated value

73

74

75

76

77

78

79

80

81 **1   Introduction**

82   Wheat germ is the name given to the embryo of the wheat seed, an important by-

83   product of the wheat milling industry. The germ represents approximately 2-3 g/100g

84   of the whole grain weight, and contains between 8-14g of oil per 100g of germ

85   (Capitani et al., 2011). Germ is considered a natural source of highly concentrated

86   nutrients such as proteins, lipids, sugars and minerals, as well natural antioxidants as

87   tocopherols,   B-group   vitamins,   carotenoids,   flavonoids,   phytosterols   and

88   policosanols.

89   Typical applications around the world are germ-enriched bread, snack foods, and

90   supplements to breakfast cereals, as well as wheat germ oil, mostly used in food,

91   medical and cosmetic industries. A high amount of wheat germ is produced annually

92   as a by-product of wheat milling industry in Argentina. In 2016 about 5.8 million

93   metric tonne (FAIM, 2017) of wheat were milled, leading to about 174,000 tonne of

94   wheat germ. Most of the germ produced is currently utilised for animal fed, though its

95   potential for human consumption is high (Ge et al., 2000), due to its remarkable

96   nutritional characteristics.

97   Wheat germ degrades rapidly, because the mechanical treatment involved in wheat

98   milling, causes the rupture of some cells and thus the spreading of the oil.

99   Degradation is mainly produced by the action of oxidative and hydrolytic enzymes

100   such as lipase and lipoxygenase on the unsaturated fatty acids chains included in the

101   lipid molecules of wheat germ (Brandolini and Hidalgo, 2012; Niu et al., 2013).

102   In order to limit the wheat germ enzymatic activity and to extend its shelf life, several

103   stabilization   processes   had   been   applied: extrusion   (Gómez   et   al.   2011),

104   microwaving (Xu et al., 2013), infrared radiation treatment (Gili et al. 2017), steaming

5

105 (Ferrara et al., 1991; Sudha et al., 2007), dehydration (Rothe, 1963) as well as

106 chemical preservation for instance by adding antioxidants (Barnes, 1948) or alkalis

107 (Grandel, 1959).

108 Fluidization provides faster mass and, particularly, energy exchange between

109 product and hot air, leading to a uniform treatment in the material being fluidised

110 (Giner and Calvelo 1987) due to the high degree of mixing inherent to the process.

111 Wheat germ flakes present good potential for fluidisation aimed at stabilising the

112 product due to its non-sticky surface and low density (Gili et al., 2017b). Yöndem-

113 Makascioğlu et al. 2005, studied wheat germ stabilisation employing a special type of

114 fluidised bed, the spouted bed, and reported an increase of the shelf life in wheat

115 germ by a factor of 20. Besides, a golden colour and a nutty flavour was imparted by

116 light roasting.

117 However, to the best of our knowledge, no mathematical modelling for fluid bed

118 drying of wheat germ has been proposed yet. The modelling and the parameters

119 obtained from the energy and mass transfer allowed us to predict process behaviour,

120 energy efficiency and optimize the thermal treatment for preservation of quality in the

121 stabilized product. In addition, modelling and simulation are important for equipment

122 design and may help industrial scaling up (Di Scala and Crapiste, 2008).

123 The dehydration stage can be studied by dividing the process conceptually into

124 simpler systems. Thin layer drying involves the study of thin product layers under

125 constant air conditions, thus all variations occur within the product and so, the drying

126 parameter thus measured can be related to those air conditions (Márquez et al.,

127 2006; Mohapatra and Rao, 2005).

128 The modelling of wheat germ thermal treatment by fluidised thin layer is the first step

129 in the way to equipment design and then its industrial implementation. A rapid

130 process is required to stabilise a material with high quality protein content, excellent

131 fatty acid profile, high tocopherol, vitamin B and dietary fiber contents, which can be

132 employed as a nutritionally-rich ingredient for foods, thus widening the range of

133 products offered by the wheat milling industry.

134 On these grounds, the aim of this work was to study the mass and energy exchange

135 of wheat germ in fluidised bed dryers by applying analytical solutions of the diffusion

136 equation, solving the macroscopic energy balance and to compare the predictions

137 with the experimental results.

138

139 **2 Materials and methods**

140 **2.1 Materials**

141 Wheat germ samples were provided by a local company (José Minetti y Cia. Ltda.

142 S.A.C.I, Córdoba, Argentina) after grain milling (2015 harvest).

143

144 **2.2 Preliminary operations**

145 A sieving stage was utilized to separate the bran and flour fraction from wheat germ

146 particles (EJR 2000, Zonytest®). Once the wheat germ particles were separated

147 (93.3% in mass retained on 20 mesh-size (0.841 mm)), they were stored at −18°C in

148 a three-layer package (polyester, aluminium and polyethylene) with barriers against

149 oxygen and light until further use. The frozen storage process of wheat germ

150 particles produces a negligible effect on its physical properties. In a previous study,

7

151 the dimensions of wheat germ particles where determined: they had a flat ellipsoidal

152 shape, an effective diameter of particle of 0.623±7.45 x10^{-8} mm, a major axis of

153 2.28±0.31 mm, a minor axis of 1.59±0.24 mm. The thickness was 0.29±0.03 mm (Gili

154 et al., 2017b).

155

156 **2.3 Moisture content**

157 Moisture content was analysed according to standard method of American

158 Association of Cereal Chemists (2012).

159

160 **2.4 Fluidised bed equipment**

161 The equipment used was a purpose-built fluidised-bed dryer, built in the workshop of

162 the Faculty of Engineering, National University of La Plata, Argentina (Torrez Irigoyen

163 and Giner, 2011). It is composed of (i) a thermally insulated drying chamber, 0.10 m

164 internal diameter and 0.30 m in height with a double glazing inspection window made

165 of borosilicate glass, (ii) a Testo 435 hot wire anemometer to measure air velocity

166 upstream the chamber in cold airflow through a duct 1 m in length (0- 20 m/s, with an

167 error of 0.03 m/s), (iii) a Testo 525 micromanometer (0–25 hPa, with an error of 0.2%

168 at full scale) to measure pressure differences through the bed, (iv) an electronic

169 temperature controller which include a software developed in Java language that

170 allows the temperature of the air entering the chamber to be set (inlet air

171 temperature), (v) a centrifugal fan, powered with a Siemens 0.55 kW electric motor

172 (maximum angular speed, 2800 RPM), (vi) a WEG (Model CFW-08, Brazil) variable-

173 frequency drive to control the air velocity by regulating the angular fan speed, and

174 (vii) two U-shaped nickel-plated copper resistance, 8 mm in diameter each, forms the

175 resistor bank, capable to heat the air up to 325 °C.

176

2.5 Thin-layer drying in fluidised bed

178 The wheat germ minimum fluidisation velocity was previously determined (0.35±0.02

179 m/s) (Gili et al., 2017b).The drying process was performed with inlet air temperature

180 of 90°C, 110°C, 130°C and 150°C using an average air velocity of 0.50±0.05 m/s,

181 approximately 1.5 minimum fluidisation velocity, was used in order to have realistic

182 results because this value is the operational velocity employed in thick fluidized beds.

183 The wheat germ samples were spread on the drying chamber in a thin layer (0.03 m).

184 The bed thickness did not alter the thin layer essence of the system because the air

185 velocity is about ten times as high as in fixed bed drying.(Torrez Irigoyen and Giner,

186 2014).

187 Samples were treated at several times between 0.5 and 15 min in duplicate. After

188 each period, samples were placed in sealed packages and stored under refrigeration.

189 Temperature measurements were taken during treatment with an infrared

190 thermometer Testo 832 T2 (Testo AG, Germany) being each experimental value the

191 average of three readings.

192

3 Mathematical modelling of thin layer drying

194

195 **3.1 Microscopic mass balance with diffusional transport of water**

196 Assuming water transport by molecular diffusion and considering the wheat germ

197 flake volume as a system, the microscopic mass balance can be expressed, for

198 constant volume of wheat germ, as: (Crank, 1975)

199 $\frac{\partial W_i}{\partial t} = \nabla\left(D_{eff} \nabla W_i\right)$ Eq. (1)

200 where D_{eff} is the effective diffusion coefficient of water relative to the dry matter.

201 As to the wheat germ particle had a flat ellipsoidal shape, a unidimensional water flux

202 in slab geometry and constant diffusion coefficient, i.e. independent of moisture

203 content was considered in agreement with Ruhanian and Movagharnejad (2016), Eq.

204 (1) can be mathematically developed to give:

205 $\frac{\partial W_l}{\partial t} = D_{eff}\left(\frac{\partial^2 W_l}{\partial l^2}\right)$ Eq (2)

206 This equation applies in each internal point of the solid, and provides the local

207 moisture content of the diffusing component W_l as a function of the time t and the

208 linear coordinate l, normal to the surface and, whose origin is placed at the centre of

209 the slab.

210

211 **3.2 Initial and boundary conditions in mass transfer**

212 To solve the partial differential equation Eq. (2), the initial and boundary conditions

213 were the following:

214 **3.2.1 Initial condition**

215 $t = 0$ $W_l = W_0$ $0 \leq l \leq L_0$ Eq (3)

216   where L_0 is the half thickness of the wheat germ particle ($2L_0$) corresponding to the

217   initial moisture content W_0.

218

3.2.2 Boundary condition at the centre

220   At the centre of the slab, the water flux is zero by symmetry

221    $l = 0 \qquad \dfrac{\partial W_l}{\partial l} = 0 \qquad t > 0$ Eq. (4)

3.2.3 Boundary conditions at the surface

223   At the surface, the convective outflow through the surrounding boundary layers to the

224   hot air is equal to the diffusive water flux from the inside of the particle to the surface

225    $-\rho_{s0} D_{eff} \dfrac{\partial W_l}{\partial l} = k_p (p_{vs} - p_{va})$ Eq. (5)

226   A progressive decrease of p_{vs} towards p_{va}, or, in equivalent terms, a gradual

227   decrease of the surface moisture content (W_s) towards the equilibrium value (W_e),

228   calculated by sorption isotherm at the temperature and relative humidity of the drying

229   air (Giner and Mascheroni, 2001), was postulated in the general surface condition

230   presented by Eq. (5).

231   When the internal control of mass transfer is dominant, large mass transfer Biot

232   numbers (Bi_m) are expected and the general surface condition presented by Eq. (5)

233   reduces to a prescribed value:

234    $l = L_0 \qquad W_s = W_e \qquad t > 0$ Eq.(6)

235   Where W_s is the particular value of W_l at the surface. Considering the high air

236   velocities employed during wheat germ thermal treatment by fluidisation, the external

237 resistance may be considered negligible compared to the internal, thus implying a

238 strict internal control for mass transfer. (Torrez Irigoyen and Giner 2014).

239

240 **3.3 Analytical solution of the diffusion equation**

241 The initial condition given by Eq. (3) and boundary conditions of Eq. (4) and (6), with

242 the unsteady state diffusion model for plane sheet (Eq. (2)),can be analytically solved

243 after integration in the solid volume to provide the mean moisture content W_m as a

244 function of time (Crapiste and Rotstein 1997; Doymaz and Osman 2010; Vega-

245 gálvez et al. 2011).

246 $$W_{ad} = \frac{W_m - W_e}{W_0 - W_e} = \frac{8}{\pi^2} \sum_{n=0}^{n=\infty} \frac{1}{(2n+1)^2} \exp\left[-\frac{(2n+1)^2 \pi^2}{4}\left(\frac{D_{eff} t}{L_0^2}\right)\right]$$ Eq. (7)

247 where W_{ad} is the dimensionless moisture content, or moisture ratio (Ah-Hen et al.,

248 2013; Akpinar and Bicer, 2005). The group $D_{eff} t / L_0^2$ is the dimensionless time or

249 Fourier number for mass transfer (Fo).

250 Becker (1959) has defined the dimensionless time as $X^2 = A_v^2 D_{eff} t$ being A_v the

251 surface area per unit volume or $1/L_0$ for an slab geometry. So, replacing $D_{eff} t / L_0^2$ in

252 Eq. (7) in term of as X^2 yields

253

254 $$W_{ad} = \frac{W_m - W_e}{W_0 - W_e} = \frac{8}{\pi^2} \sum_{n=0}^{n=\infty} \frac{1}{(2n+1)^2} \exp\left[-\frac{(2n+1)^2}{4} \pi^2 X^2\right]$$ Eq. (8)

12

255 To obtain the solution with the infinite series. a considerable number of terms is

256 required to converge, particularly at short times. However, for long times, only one

257 term of the infinite series suffices for convergence ($W_{ad} < 0.3$ or $X > 1$).

258 **3.4 Approximate analytical solution of the diffusion equation**

259 A simpler solution (Eq. (9)) of the diffusion equation proposed by Becker (1959) was

260 used to estimate the drying curve at short dimensionless times ($X \leq 1$) without losing

261 the accuracy of the full series solution (Eq. (8)) for the slab. The expression is:

262 $$W_{ad} = \frac{W_m - W_e}{W_0 - W_e} = 1 - \frac{2}{\sqrt{\pi}} A_v \sqrt{D_{eff} \, t} \qquad \text{Eq. (9)}$$

263 This type of solution was successfully applied for spherical geometry in other drying

264 studies to predict grain drying curves.(M. C. Gely and Giner 2007; R. M. Torrez

265 Irigoyen and Giner 2014). In the present study, this mathematical expression (Eq.

266 (9)) was fitted to experimental data considering the half thickness of the particle at

267 the initial moisture content (L_0).

268 The root mean square error of the estimate was calculated as:

269 $$S_y = \sqrt{\frac{\sum_{i=1}^{i=n} (y_{exp,i} - y_{pred,i})^2}{n-1}} \qquad \text{Eq. (10)}$$

270

271 Where $y_{exp,i}$ and $y_{pred,i}$ are the experimental and predicted values respectively,

272 corresponding to the same treatment time.

273

274 **3.5 Macroscopic energy balance**

275

13

276 The wheat germ particle temperature is assumed to be uniform, i.e. the internal

277 temperature profile in the particle is flat, although variable with time (Rodríguez-

278 Fernández et al., 2007). This characteristic is due heat transfer Biot number, which

279 tends to zero with the progress of drying (Giner et al., 2010). Therefore, a

280 macroscopic energy balance was applied to the wheat germ particle, considering that

281 the heat exchange between particle and air was regulated by an external control:

282 $\rho_s C_p \frac{dT}{dt} = h_T A_v (T_a - T) - \rho_s \left(-\frac{dW_m}{dt}\right) L_g$ Eq. (11)

283

284 Where A_v is the specific particle surface (surface area/volume), T_a is the drying air

285 temperature and $(-dW_m/dt)$ is the drying rate, based on the average moisture

286 content, calculated from experimental data using a finite difference approximation.

287 The initial condition for the heat transfer equation obtained is $(t = 0)$ $T = T_0$. In this

288 ordinary differential equation, the derivatives are total since, as mentioned earlier, the

289 temperature gradient within the product is assumed negligible while W_m is an

290 average value spatially integrated in the particle (Rahman and Kumar, 2006; Torrez

291 Irigoyen et al., 2014). It is important to highlight that the heat capacity (C_p) of wheat

292 germ particle is based on the product dry mass (J/ kg dry matter °C), though it is

293 nonetheless a function of the average moisture content of the particle.

294 The specific heat of particle was calculated from (Mohsenin, 1980) (Eq. (11)), for

295 moisture content up to 0.7 kg water/kg dry matter.

296

297 $C_p = 1638.08 + 3566.19 \, W_m$ Eq. (12)

298

14

299   The energy balance was solved by utilizing the specific heat, calculated at every

300   moment of the treatment, employing the average moisture content of the

301   particle.(Torrez Irigoyen et al., 2014)

302

3.5.1   Heat of desorption

304

305   The enthalpy or heat of water desorption of wheat germ particle can be estimated

306   with an expression deduced from the Clapeyron equation and a model for the

307   sorption isotherm (Chen, 2006; Chenlo et al., 2011; Giner and Gely, 2005):

308

309     $L_g = \frac{RT_k^2}{M_w}\left[\frac{d(Ln(p_s))}{dT_k} + \left(\frac{\partial(Ln(a_w))}{\partial T_k}\right)_w\right]$ Eq. (13)

310

311   By operating mathematically on the right hand side of the equal sign in Eq. (13), we

312   can find

313     $L_g = L_w + \frac{R_g T_k^2}{M_w}\left(\frac{\partial(Ln(a_w))}{\partial T_k}\right)_w$ Eq. (14)

314   Where the first term of the right hand side of the equal sign is the heat of vaporization

315   of water, while the factor $(\partial Ln(a_w)/\partial T_k)_w$ is calculated using a sorption isotherm

316   equation The heat of desorption was taken as equal to L_w, following the criterion

317   adopted by R. M. Torrez Irigoyen et al., (2014) for soybeans.

318 **3.5.2 Determination of the effective heat transfer coefficient during the thermal**

319   **treatment of wheat germ by fluidisation**

320 The macroscopic energy balance (Eq. (11)) is an ordinary differential equation solved

321 by the Euler method using short times steps (T) were compared with the

322 experimental thermal histories and, the residuals transferred to an optimization

323 procedure of determination of h_t by minimization the sum of residuals squared

324 (Eq.(15)).(Torrez Irigoyen et al., 2014)

325 $$SSR = \sum_{i=1}^{N}(T_{exp,i} - T_i)^2 \hspace{3cm} \text{Eq. (15)}$$

326 Predictions errors were determined from the results of the fitting procedure by

327 employing the absolute average deviation (AAD) (Eq. 16). Hence, errors were

328 obtained in the same units as the dependent variable. The corrected coefficient of

329 determination (r^2) was also calculated as an index of goodness of fit (Torrez Irigoyen

330 et al., 2014).

331

332 $$AAD = \frac{1}{n}\sum_{i=1}^{n}\left|y_{exp,i} - y_{sim,i}\right| \hspace{3cm} \text{Eq. (16)}$$

333 Where $y_{exp,i}$ and $y_{sim,i}$ are the experimental and simulated values.

334

335 **4   Results and discussion**

336 **4.1   Experimental thin-layer drying curves in fluidised bed**

337 The thermal treatment of wheat germ was carried out in a dryer at 90°C, 110°C,

338 130°C and 150°C using an average air velocity of 0.50 m/s. The experimental thin-

16

339   layer curves can be observed in Fig. 1 where the measured dimensionless moisture

340   content (W_{ad}) was plotted as a function of time.

341   W_{ad} was calculated as indicated in the left term of Eq. (7) where W_0 is the initial

342   moisture content of the particle, W_m is the mean moisture content of wheat germ

343   particle at time t, and W_e is the equilibrium moisture content measured in an extra-

344   long treatment ($t > 3600\,s$) carried out for each air temperature to consider the

345   different relative humidity values at the various air temperatures used

346   An abrupt decrease of W_{ad} with time was found (Fig. 1). As expected, higher air

347   temperatures led to higher absolute drying rates. The nonlinear behaviour of the

348   curve and the fast evaporation of water from the surface of the particle indicated that

349   wheat germ drying can be taken to occur during the falling drying rate period.

350

351   **4.2 Approximate analytical solution of the diffusion equation**

352   The Becker model (Eq. (9)), as mentioned before, is applicable to estimate the thin-

353   layer drying curve in the range of $0.3 < W_{ad} < 1$ without losing the infinite series

354   accuracy. This model was fitted to the experimental data of Fig. 1 by using a

355   nonlinear least squares method (Systat, 1990). The parameters thus obtained and

356   the statistical indexes of goodness of fit are presented in Table 1, while the predicted

357   drying curves are depicted in Fig. 2.

358   As Fig. 2 shows, the short times equation (Eq. (9)) kept a good agreement with

359   experimental data up to values of Wad of 0.2-0.3 despite the elevated air

360   temperatures utilized during the treatments. The model was outside its applicability

361   range for $W_{ad} < 0.3$ and the calculated values did not provide a good representation

17

362 of observed values and, moreover, predicted negative values of dimensionless

363 moisture content, which is physically absurd.

364 Based on the results obtained, the Becker model was inadequate to predict the entire

365 thermal treatment of wheat germ particles in fluidised bed as a thin layer-drying

366 equation for the thermal treatment applied to wheat germ particles. Due to the high

367 inlet air temperatures utilized, at 150°C only a few points were correctly predicted by

368 the Becker model. Comparable results were informed by R. M. Torrez Irigoyen and

369 Giner (2014) for drying-toasting of presoaked soybean.

370 **4.3 Analytical solution of the diffusion equation**

371

372 In view of on the unsuitable fitting presented by the approximate analytical solution

373 (Eq. (9)) for the all experimental data obtained at the several air temperatures, the

374 complete analytical solution of the diffusion equation (Eq. (7)) was finally applied to

375 predict the behaviour of the thermal treatment. The convergent infinite series (Eq.

376 (7)) was fitted to the experimental data (Systat, 1990) by nonlinear square method.

377 Eleven terms from n=0 until n=10 of the analytical solution were used in the fitting,

378 which ensures practical convergence at all times. This criterion was maintained in all

379 thermal treatments.

380 Fig. 3 shows the experimental dimensionless moisture contents and predicted values

381 by Eq. (7) as a function of time over the four thermal treatments. The complete

382 analytical solution described the sets of experimental data satisfactorily at each air

383 temperature, and the diffusion coefficients obtained were similar to those reported in

384 vegetables, seeds and grains (Gely and Santalla, 2007; Torrez Irigoyen and Giner,

385 2014; Vega-gálvez et al., 2011).

18

386   The accurate predictions of dimensionless moisture content were obtained in spite of

387   the assumptions made of constant diffusion coefficient and constant particle volume,

388   which are required for developing complete analytical solution (Crank, 1975).

389   Although such premises for the analytical solution were not strictly realistic, the good

390   prediction given by the model may be explained by the ratio D_{eff}/L_0^2 which keeps

391   substantially constant in the equation.(Torrez Irigoyen and Giner, 2014).The results

392   obtained from the fitting procedure and the statistical parameters of goodness of fit

393   are shown in Table 2. Water diffusivity values determined here are comparable to

394   3.7×10^{-12}- 2.32×10^{-11} (m^2/s) for air drying of quinoa at 60°C-90°C (Gely and Santalla,

395   2007), 7.76×10^{-10} – 9.35×10^{-9} (m^2/s) for carrots for air drying of carrot cubes at 50°C-

396   70°C (Doymaz, 2004), 8.21×10^{-10} – 2.61×10^{-9} (m^2/s) for fluidised bed drying of castor

397   oil seed at 90 °C and 110°C (Perea-Flores et al., 2012), and 1.39×10^{-11} – 3.94×10^{-11}

398   (m^2/s) for spouted fluidised bed drying of barley at 36°C-56°C (Markowski et al.,

399   2010). These values are consistent with the wheat germ diffusion coefficients

400   estimated in the present work.

401

402   **4.4   Dependence of diffusion coefficient with temperature**

403

404   The dependence of the effective diffusion coefficient with temperature was studied

405   for several authors in food drying (Gely and Giner, 2007; Guiné et al., 2012; Perea-

406   Flores et al., 2012). An increase in the temperature speeds up molecular diffusion,

407   and this effect is represented by a rise of the diffusion coefficient. A relationship with

408 the inlet air temperature of the fluidised bed dryer can be described by an Arrhenius-

409 type equation as follows:

410 $Ln(D_{eff}) = Ln(D_\infty) - \frac{E_a}{R(T_a + 273.15)}$ Eq. (17)

411 Where D_∞ (m^2/s) is factor equivalent to the diffusivity at infinitely high temperature, E_a

412 (J/mol) is the activation energy, a measure of the effect of temperature on the

413 diffusion coefficient (related with the binding energy of between water and material)

414 and R (8.314 x10^{-3} kJ/mol K) is the universal gas constant.(Perea-Flores et al., 2012).

415 An Arrhenius-type equation (Eq. (17)) was fitted to the diffusivities for each air

416 temperature in order to determine E_a and D_∞. The predictions for the data obtained

417 from the complete analytical solution (Eq. (7)) were showed in Table 2.

418 The activation energy (39.27 kJ/mol) was comparable to values reported by other

419 researchers who studied diverse conditions of food drying (Guiné et al., 2012; Perea-

420 Flores et al., 2012; Torrez Irigoyen and Giner, 2014; Zielinska and Markowski, 2007).

421

422 **4.5 Determination of the effective heat transfer coefficient**

423

424 The effective heat transfer coefficient was determined from macroscopic balance of

425 energy (Eq. (11)). To solve the Eq. (11) the C_p and L_g were estimated according to

426 Eq. (12) and (15). The wheat germ particle density (ρ_p) value utilized was 1234.23

427 kg/m^3 (Kim et al., 2003). The estimated heat transfer coefficients ranged between

428 7.87 and 16.55 W/m^2°C (Table 3). These results were lower than the coefficients

429 determined by R. M. Torrez Irigoyen et al. (2014) during drying-toasting of presoaked

430   soybean but were in the same range that values found for carrots by Zielinska and

431   Markowski (2007).

432   The experimental and the predicted surface temperatures showed a reasonable

433   agreement for all the air temperatures analysed (Fig. 4). Predicted curves somewhat

434   overestimates the experimental temperature between 100 and 200 s. Particles were

435   heated very fast; in fact, in a time shorter than 300 s the temperature of germ

436   particles were close to the asymptotic or equilibrium air value. This abrupt approach

437   of the particle temperature to the equilibrium temperature is explained by the intense

438   heat exchange between air and particles that occurs during the fluidised bed

439   process, due to the high degree of mixing experienced by particles inside the drying

440   chamber. Furthermore, it is important to note that neither the shape of the

441   experimental moisture curves (Fig. 1) nor the temperature heating profile of wheat

442   germ particles (Fig. 4) denotes the presence of a constant drying rate period which

443   indicates that the internal control considered in the model was appropriate.

444   **5   Conclusion**

445   In the present work, a thin layer mathematical model of heat and mass transfer for

446   the thermal treatment of wheat germ, carried out at 90°C, 110°C, 130°C and 150°C,

447   was applied to data in order to improve the understanding of this process that

448   stabilizes germ particles as an ingredient for human consumption.

449   The moisture loss was observed to occur in the falling drying rate period. A strict

450   internal control to the mass transfer rate, constant diffusion coefficient and constant

451   particle volume was assumed to apply analytical solutions for unsteady state

452   diffusion in a slab

21

453 The approximate analytical solution for short times or Becker model was unsuitable

454 to describe the complete drying process at the high air temperatures used . On the

455 other hand, the complete analytical series solution of the diffusion equation was able

456 to describe with reasonable accuracy the experimental data of drying for all air

457 temperatures

458 The experimental diffusion coefficients determined in this study were within the range

459 expected for water diffusion in solids despite at the high temperatures used. Their

460 dependence with air temperature was described by an Arrhenius-type equation. The

461 activation energy (about 39 kJ/mol) was within the range expected for the drying of

462 solid foods.

463 A macroscopic energy balance was solved to predict the transient temperature curve.

464 By fitting the results of the numerical solution of this equation to the experimental

465 data, the effective heat transfer coefficients were determined to each temperature

466 analysed.

467 Both predicted dimensionless moisture contents and surface temperature of wheat

468 germ as a function of time were in good agreement with the meas experimental

469 measures.

470 The outcome of this study may be would be utilized in future work to relate thermal

471 treatment, drying curve and the protective effect on nutritional quality for wheat germ

472 particles both for human consumption or as raw material for the cosmetic industry.

473

475

7   References

482 AOCS (2009) Official methods and recommended practices of the American Oil

484   Chemists' Society (5th ed.). Champaign, Illinois, USA.

485 AACC International, 2012. Approved Methods of Analysis, Method 44-15.02.

486   Moisture – air-oven methods. St. Paul, MN, USA. doi:10.1094/ AACCIntMethod-

487   44-15.02.

488 Ah-Hen, K., Zambra, C.E., Aguëro, J.E., Vega-Gálvez, A., Lemus-Mondaca, R.,

489   2013. Moisture Diffusivity Coefficient and Convective Drying Modelling of Murta

490   (Ugni molinae Turcz): Influence of Temperature and Vacuum on Drying Kinetics.

491   Food Bioprocess Technol. 6, 919–930. doi:10.1007/s11947-011-0758-5

492 Akpinar, E.K., Bicer, Y., 2005. Modelling of the drying of eggplants in thin-layers. Int.

493   J. Food Sci. Technol. 40, 273–281. doi:10.1111/j.1365-2621.2004.00886.x

494 Barnes, H.M., 1948. Process of stabilizing organic materials and products of said

495   process. US 2448208 A.

496 Becker, H.A., 1959. A study of diffusion in solids of arbitrary shape, with application

497   to the drying of the wheat kernel. J. Appl. Polym. Sci. 1, 212–226.

498   doi:10.1002/app.1959.070010212

499 Brandolini, A., Hidalgo, A., 2012. Wheat germ: not only a by-product. Int. J. Food Sci.

500   Nutr. 63, 71–74. doi:10.3109/09637486.2011.633898

501 Capitani, M., Mateo, C.M., Nolasco, S.M., 2011. Effect of temperature and storage

502   time of wheat germ on the oil tocopherol concentration. Brazilian J. Chem. Eng.

503   28, 243–250. doi:10.1590/S0104-66322011000200008

504 Chen, C., 2006. Obtaining the isosteric sorption heat directly by sorption isotherm

505   equations. J. Food Eng. 74, 178–185. doi:10.1016/j.jfoodeng.2005.01.041

506   Chenlo, F., Moreira, R., Prieto, D.M., Torres, M.D., 2011. Desorption Isotherms and

507   Net Isosteric Heat of Chestnut Flour and Starch. Food Bioprocess Technol. 4,

508   1497–1504. doi:10.1007/s11947-009-0239-2

509   Crank, J., 1975. The mathematics of diffusion, Oxford University Press. Oxford

510   University Press. doi:10.1016/0306-4549(77)90072-X

511   Crapiste, G.H., Rotstein, E., 1997. Design and Performance Evaluation of Dryers, in:

512   Rotstein, E., Singh, R.P., Valentas, K.J. (Eds.), Handbook of Food Engineering

513   Practice. CRC Press, Ney York, p. 699.

514   Di Scala, K., Crapiste, G., 2008. Drying kinetics and quality changes during drying of

515   red pepper. LWT - Food Sci. Technol. 41, 789–795.

516   doi:10.1016/j.lwt.2007.06.007

517   Doymaz, I., 2004. Convective air drying characteristics of thin layer carrots. J. Food

518   Eng. 61, 359–364. doi:10.1016/S0260-8774(03)00142-0

519   Doymaz, I., Osman, I., 2010. Drying characteristics of sweet cherry. Food Bioprod.

520   Process. 9, 31–38. doi:10.1016/j.fbp.2010.03.006

521   FAIM, 2017. Molienda y producción de Harina [WWW Document].

522   Ferrara, P.J., Ridge, R.D., Benson, J.T., 1991. Method of producing shelf stable

523   wheat germ. US Pat 5.063.079.

524   Garza, S., Ibarz, A., Pagán, J., Giner, J., 1999. Non-enzymatic browning in peach

525   puree during heating. Food Res. Int. 32, 335–343. doi:10.1016/S0963-

526   9969(99)00094-0

527 Ge, Y., Sun, A., Ni, Y., Cai, T., 2000. Some nutritional and functional properties of

528   defatted wheat germ protein. J. Agric. Food Chem. 48, 6215–6218.

529   doi:10.1021/jf000478m

530 Gely, M.C., Giner, S.A., 2007. Diffusion Coefficient Relationships during Drying of

531   Soya Bean Cultivars. Biosyst. Eng. 96, 213–222.

532   doi:10.1016/j.biosystemseng.2006.10.015

533 Gely, M.C., Santalla, E.M., 2007. Moisture diffusivity in quinoa (Chenopodium quinoa

534   Willd.) seeds: Effect of air temperature and initial moisture content of seeds. J.

535   Food Eng. 78, 1029–1033. doi:10.1016/j.jfoodeng.2005.12.015

536 Gili, R.D., Palavecino, P.M., Cecilia Penci, M., Martinez, M.L., Ribotta, P.D., 2017a.

537   Wheat germ stabilization by infrared radiation. J. Food Sci. Technol. 54, 71–81.

538   doi:10.1007/s13197-016-2437-z

539 Gili, R.D., Torrez Irigoyen, R.M., Penci, M.C., Giner, S.A., Ribotta, P.D., 2017b.

540   Physical characterization and fluidization design parameters of wheat germ. J.

541   Food Eng. 212, 29–37. doi:10.1016/j.jfoodeng.2017.05.011

542 Giner, S.A., Calvelo, A., 1987. Modelling of wheat drying in fluidized beds. J. Food

543   Sci. 52, 1358–1363. doi:10.1111/j.1365-2621.1987.tb14082.x

544 Giner, S.A., Gely, M.C., 2005. Sorptional parameters of sunflower seeds of use in

545   drying and storage stability studies. Biosyst. Eng. 92, 217–227.

546   doi:10.1016/j.biosystemseng.2005.06.002

547 Giner, S.A., Irigoyen, R.M.T., Cicutt??n, S., Fiorentini, C., 2010. The variable nature

548   of Biot numbers in food drying. J. Food Eng. 101, 214–222.

549   doi:10.1016/j.jfoodeng.2010.07.005

550   Giner, S.A., Mascheroni, R.H., 2002. Diffusive Drying Kinetics in Wheat, Part 2:

551   applying the Simplified Analytical Solution to Experimental Data. Biosyst. Eng.

552   81, 85–97. doi:10.1006/bioe.2001.0004

553   Giner, S.A., Mascheroni, R.H., 2001. Diffusive drying kinetics in wheat, Part 1:

554   Potential for a simplified analytical solution. Biosyst. Eng. 80, 351–364.

555   doi:10.1006/bioe.2002.0066

556   Gómez, M., González, J., Oliete, B., 2012. Effect of Extruded Wheat Germ on Dough

557   Rheology and Bread Quality. Food Bioprocess Technol. 5, 2409–2418.

558   doi:10.1007/s11947-011-0519-5

559   Grandel, F., 1959. Process of making germ flakes. US Pat 2879167 A.

560   Guiné, R.P.F., Henrriques, F., Barroca, M.J., 2012. Mass Transfer Coefficients for the

561   Drying of Pumpkin (Cucurbita moschata) and Dried Product Quality. Food

562   Bioprocess Technol. 5, 176–183. doi:10.1007/s11947-009-0275-y

563   Jha, P.K., Kudachikar, V.B., Kumar, S., 2013. Lipase inactivation in wheat germ by

564   gamma irradiation. Radiat. Phys. Chem. 86, 136–139.

565   doi:10.1016/j.radphyschem.2013.01.018

566   Kim, Y.S., Flores, R.A., Chung, O.K., Bechtel, D.B., 2003. Physical, chemical, and

567   thermal characterization of wheat flour milling coproducts. J. Food Process Eng.

568   26, 469–488. doi:10.1111/j.1745-4530.2003.tb00613.x

569   Markowski, M., Białobrzewski, I., Modrzewska, A., 2010. Kinetics of spouted-bed

570   drying of barley: Diffusivities for sphere and ellipsoid. J. Food Eng. 96, 380–387.

571   doi:10.1016/j.jfoodeng.2009.08.011

572   Márquez, C.A., De Michelis, A., Giner, S.A., 2006. Drying kinetics of rose hip fruits

573   (Rosa eglanteria L.). J. Food Eng. 77, 566–574.

574   doi:10.1016/j.jfoodeng.2005.06.071

575   Mohapatra, D., Rao, P.S., 2005. A thin layer drying model of parboiled wheat. J.

576   Food Eng. 66, 513–518. doi:10.1016/j.jfoodeng.2004.04.023

577   Mohsenin, N.N., 1980. Thermal Properties of Food and Agricultural Materials.

578   Gordon and Breach, Science Publishers, Ney York.

579   Niu, L.-Y., Jiang, S.-T., Pan, L.-J., Pang, M., 2013. Characterization of Wheat Germ

580   Oil in Terms of Volatile Compounds, Lipid Composition, Thermal Behavior, and

581   Structure. Int. J. Food Prop. 16, 1740–1749.

582   doi:10.1080/10942912.2011.608141

583   Perea-Flores, M.J., Garibay-Febles, V., Chanona-Pérez, J.J., Calderón-Domínguez,

584   G., Méndez-Méndez, J. V., Palacios-González, E., Gutiérrez-López, G.F., 2012.

585   Mathematical modelling of castor oil seeds (Ricinus communis) drying kinetics in

586   fluidized bed at high temperatures. Ind. Crops Prod. 38, 64–71.

587   doi:10.1016/j.indcrop.2012.01.008

588   Rahman, N., Kumar, S., 2006. Evaluation of convective heat transfer coefficient

589   during drying of shrinking bodies. Energy Convers. Manag. 47, 2591–2601.

590   doi:10.1016/j.enconman.2005.10.025

591   Rodríguez-Fernández, M., Balsa-Canto, E., Egea, J.A., Banga, J.R., 2007.

592   Identifiability and robust parameter estimation in food process modeling:

593   Application to a drying model. J. Food Eng. 83, 374–383.

594   doi:10.1016/j.jfoodeng.2007.03.023

595   Rothe, M., 1963. Uber ein neues Stabilisierungsverfahren fur Weizenkeime. Mol.

596   Nutr. Food Res. 7, 579–587. doi:10.1002/food.19630070805

597   Ruhanian, S., Movagharnejad, K., 2016. Mathematical modeling and experimental

598   analysis of potato thin-layer drying in an infrared-convective dryer. Eng. Agric.

599   Environ. Food 9, 84–91. doi:10.1016/j.eaef.2015.09.004

600   Sudha, M.L., Srivastava, A.K., Leelavathi, K., 2007. Studies on pasting and structural

601   characteristics of thermally treated wheat germ. Eur. Food Res. Technol. 225,

602   351–357. doi:10.1007/s00217-006-0422-x

603   Torrez Irigoyen, R.M., Giner, S.A., 2014. Drying-toasting kinetics of presoaked

604   soybean in fluidised bed. Experimental study and mathematical modelling with

605   analytical solutions. J. Food Eng. 128, 31–39.

606   doi:10.1016/j.jfoodeng.2013.12.009

607   Torrez Irigoyen, R.M., Giner, S.A., 2011. Fluidisation velocities during processing of

608   whole soybean snack. J. Food Eng. 107, 90–98.

609   doi:10.1016/j.jfoodeng.2011.05.040

610   Torrez Irigoyen, R.M., Goñi, S.M., Giner, S.A., 2014. Drying-toasting kinetics of

611   presoaked soybean. A mathematical model considering variable diffusivity,

612   shrinkage and coupled heat transfer. J. Food Eng. 142, 70–79.

613   doi:10.1016/j.jfoodeng.2014.06.002

614   Vega-gálvez, A., Dagnino-subiabre, A., Terreros, G., López, J., Miranda, M., Scala,

615   K. Di, 2011. Mathematical Modeling of Convective Air Drying of Quinoa-

616   Supplemented Feed for Laboratory Rats 54, 161–171.

617   Xu, B., Zhou, S.L., Miao, W.J., Gao, C., Cai, M.J., Dong, Y., 2013. Study on the

618   stabilization effect of continuous microwave on wheat germ. J. Food Eng. 117,

619   1–7. doi:10.1016/j.jfoodeng.2013.01.031

620   Yöndem-Makascioğlu, F., Gürün, B., Dik, T., Kincal, N.S., 2005. Use of a spouted

621   bed to improve the storage stability of wheat germ followed in paper and

622   polyethlyene packages. J. Sci. Food Agric. 85, 1329–1336.

623   doi:10.1002/jsfa.2102

624   Zielinska, M., Markowski, M., 2007. Drying Behavior of Carrots Dried in a Spout–

625   Fluidized Bed Dryer. Dry. Technol. 25, 261–270.

626   doi:10.1080/07373930601161138

627

Table 1. Diffusion coefficients resulting from fitting Eq. (9) to experimental data of Fig. (1) ($W_{ad} \geq 0.3$) and their associated errors, the coefficient of determination (r^2) and root mean square error of the estimate (S_y).

Air Temperature (°C)	D_{eff} x 10^{10} (m^2/s)	r^2	S_y
90	1.1291	0.903	0.2352
110	1.7211	0.982	0.0924
130	2.2861	0.969	0.0908
150	7.5756	0.971	0.1233

Table 2. Diffusion coefficients resulting from fitting Eq. (7) to experimental data of Fig. (1) and their associated errors, the coefficient of determination (r^2) and root mean square error of the estimate (S_y). Also, the table shows the activation energy and the preexponential factor of the adjusted Arrhenius-type equation.

| Air Temperature (°C)	D_{eff} x 10^{10} (m^2/s)	r^2	S_y	E_a (kJ/mol)	D_∞ x 10^5 (m^2/s)
90	0.3220	0.942	0.2361		
110	0.4438	0.985	0.1288		
				39.27	1.144
130	0.5865	0.963	0.1127		
150	2.3768	0.990	0.0479		

Table 3. Heat transfer coefficients resulting from fitting Eq. (11) to experimental data and their absolute average deviation(AAD), the root mean square error of the estimate (S_y) and the coefficient of determination (r^2).

| Air Temperature (°C)	h_t (W/m²°C)	r^2	AAD (°C)	S_y
90	9.3192	0.824	4.6042	7.2102
110	9.4586	0.833	5.9767	11.3458
130	7.8747	0.896	6.0352	10.7551
150	16.5455	0.937	4.9280	11.5952

Figure 1. Experimental thin-layer curves during the drying-stabilization process of wheat germ particles at the temperatures of 90°C(●), 110°C(◇), 130°C (▲) and 150°C(□).
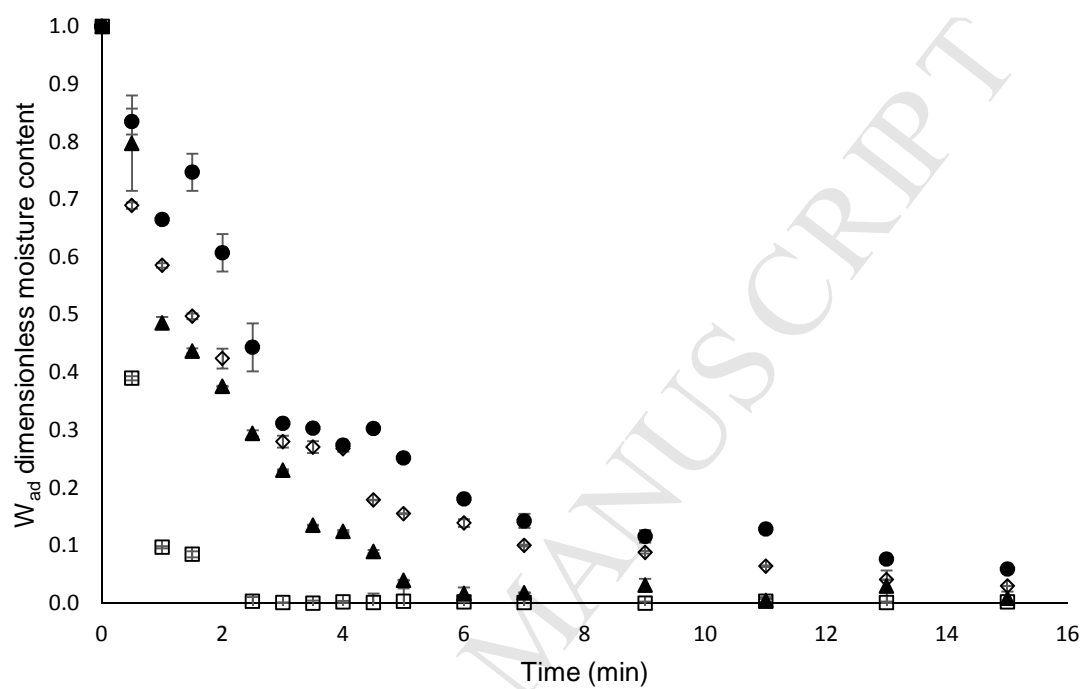
Figure 2. Thin-layer drying-stabilizing curves of wheat germ particle. Experimental data (●), and predicted values (-) by approximate analytical solution (Eq. (9)) for the inlet air temperature: (a) 90°C, (b) 110°C, (c) 130°C and (d) 150°C.
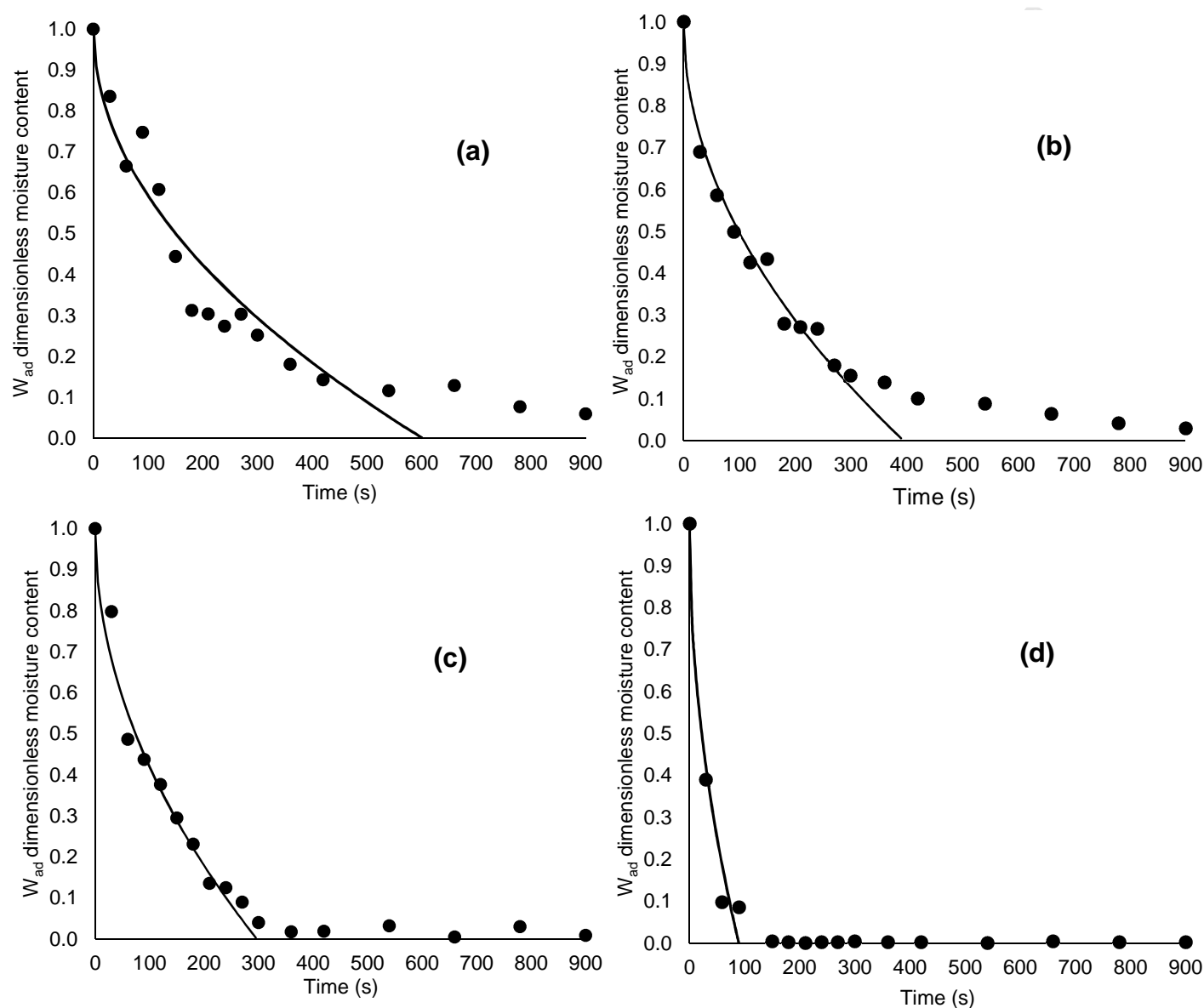
Figure 3. Thin-layer drying-stabilizing curves of wheat germ particle. Experimental data (●), and predicted values (-) by analytical solution (Eq. (7)) for the inlet air temperature: (a) 90°C, (b) 110°C, (c) 130°C and (d) 150°C.
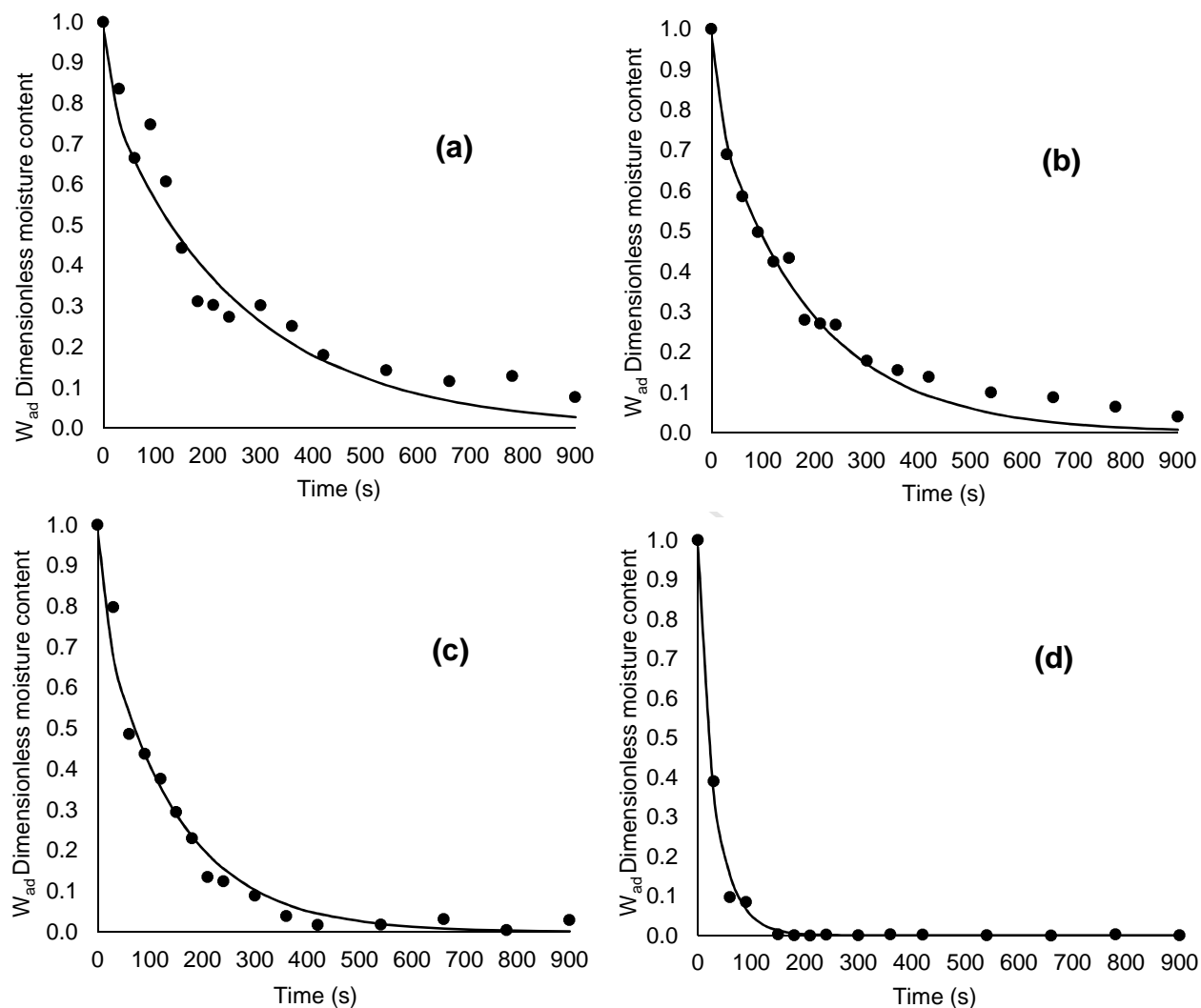
Figure 4. Wheat germ surface temperature curves as a function of drying-stabilizing time. Experimental data (▲), and predicted values (-) for the inlet air temperatures of: (a) 90°C, (b) 110°C, (c) 130°C and (d) 150°C.
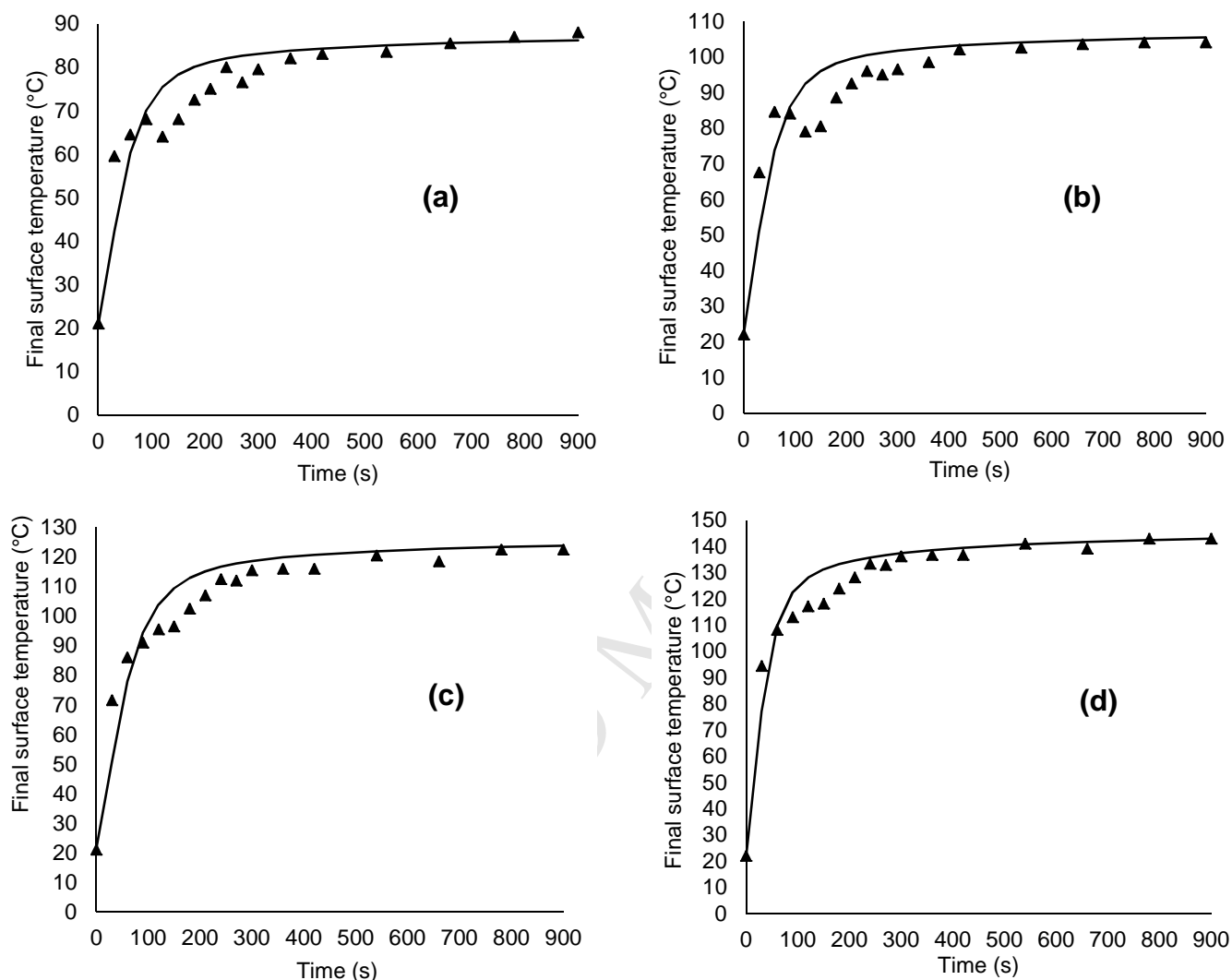
Highlights

Fluidised bed drying of wheat germ particles at 90-150°C was studied.

Two analytical solutions with constant diffusivity and constant volume were tested.

The solution for short dimensionless times was not suitable in this process.

The complete analytical solution, a series, provided excellent agreement with data.

Heat transfer coefficient and Arrhenius parameters were estimated solving inverse problems.